First comparison of array-derived rotational ground motions with direct ring laser measurements

W. Suryanto[*]   H. Igel[*]   J. Wassermann [*]   A. Cochard[*]
D. Vollmer[†]   B. Schuberth[*]   F. Scherbaum[†]   U. Schreiber[‡]
A. Velikoseltsev[‡]

October 11, 2005

Abstract

Recently, ring laser technology has provided the first consistent observations of rotational ground motions around a vertical axis induced by earthquakes. "Consistent", in this context, implies that the observed waveforms and amplitudes are compatible with collocated recordings of translational ground motions. In particular, transverse accelerations should be in phase with rotation rate and their ratio proportional to local horizontal phase velocity assuming plane wave propagation. The ring laser installed at the Fundamentalstation Wettzell in the Bavarian Forest, SE Germany, is recording the vertical component of rotation rate, theoretically a linear combination of the space derivatives of the horizontal components of motion. This suggests that, in principle, rotation can be derived from seismic array experiments by "finite-differencing". This has been attempted previously in several studies; however, the accuracy of these observations could never be tested in the absence of direct measurements. We installed a double cross-shaped array of nine stations from December 2003 to March 2004 around the ring laser instrument and observed several large earthquakes on both the ring laser and the seismic array. Here we

[1]Department of Earth and Environmental Sciences, Geophysics Section, Ludwig-Maximilians-Universität München, Theresienstr. 41, 80333, Germany
[2]Institut für Geowissenschaften, Universität Potsdam, Karl-Liebknecht-Str. 24/25, 14476 Golm, Germany
[3]Forschungseinrighung Satellitengeodäsie, Technical University of Munich, Fundamentalstation Wettzell, Sackenriederstr. 25, D-93444 Kötzting, Germany

1

present for the first time a comparison of array-derived rotations with direct measurements of rotations for ground motions induced by the $M6.4$ Al Hoceima, Morocco, earthquake of February 24, 2004. With additional synthetic seismograms we show that even low levels of noise may considerably influence the accuracy of the array-derived rotations when the minimum number of required stations (three) is used. Nevertheless – when using all nine stations – the overall fit between direct and array-derived measurements is surprisingly good (maximum correlation coefficient of 0.94).

1   Introduction

A complete representation of ground motion consists of three components of translational motion, three components of rotational motion and six components of strain (e.g., Aki and Richards 2002). Standard seismometers, however, only measure the translational components of ground motion. Even though theoretical seismologists have pointed out the potential benefits of measurements of rotational ground motion, they were not made until quite recently. Nigbor (1994) has successfully measured translational and rotational ground motion during an underground chemical explosion experiment at the Nevada Test Site using a triaxial translational accelerometer and a solid-state rotational velocity sensor. The same type of sensor was used by Takeo (1998) for recording an earthquake swarm on Izu peninsula, Japan. Moriya and Marumo (1998) introduced a rotational sensor consisting of two oppositely oriented seismometers. Teisseyre et al. (2003) used a rotational-seismograph system with two oppositely oriented seismometers, having pendulums suspended on a common axis, to record small earthquakes at Ojcow Observatory, Poland and L'Aquila Observatory, Italy.

However, the resolution of the instruments described above was too low to be applicable in seismology in a broad magnitude and distance range. Therefore, sensor developments in the past years focused on the development and refinement of optical instruments, particular using laser technology. The application of the Sagnac effect for sensing the inertial rotation using laser principles was first discussed in the sixties (Post 1967). There are two approaches to apply the Sagnac effect for rotational measurements, namely active techniques, as in ring laser gyroscopes, and passive techniques, as in fiber-optic interferometers (Sanders et al. 1981). The first application of a ring laser gyroscope as a rotational sensor in seismology was reported by Stedman et al. (1995). Further-

more, McLeod et al. (1998) gave a detailed analysis of observation with the ring laser named CI, installed in the so-called Cashmere cavern, Christchurch, New Zealand. They reported that the phase of rotation determined by CI is consistent with that of a collocated standard seismometer record, during the $M_L5.3$ Kaikoura event on September 5, 1996. Pancha et al. (2000) analyzed the horizontal and vertical components of teleseismic surface and body waves recorded by larger ring laser gyroscopes (CII and G0) caused by $M7.0$ and $M7.3$ events at distances of $31°$ and $42.6°$, respectively. Apart from amplitudes of rotation rates larger than expected, they showed – but only in a narrow frequency band – that the sensors provided sufficient accuracy to record seismic rotations. Fully consistent rotational motions were recorded by a ring laser gyro installed at the fundamental station Wettzell, Germany (Igel et al. 2005). They showed that the rotational motions were compatible with collocated recordings of transverse acceleration by a standard seismometer, both in amplitude and phase. This implies that "standard" rotational sensors with sufficient resolution may be possible in the near future.

The full benefits of the determination of rotational motion in seismology are still under investigation. Rotational motions can provide accurate data for arrival times of SH waves and, in the near-source distance range, rotational motions might provide more detailed information on the rupture processes of earthquakes (Takeo and Ito 1997). Rotational motions could also be used to better estimate the static displacement from seismic recordings, identifying translational signals cased by rotation (Trifunac and Todorovska 2001). Igel et al. (2005) introduced a method to estimate the horizontal phase velocity by using the ring laser data as well as the transverse acceleration estimated from collocated standard seismographs, whereas the standard procedure to estimate phase velocity is array measurements. Even though the comparison with theoretical predictions of phase velocities look promising (Igel et al. 2005; Cochard et al. to appear), it remains to be seen whether the estimates are accurate enough. In earthquake engineering, observations of rotational components of seismic strong motions may be of interest as this type of motion may contribute to the response of structures to earthquake-induced ground shaking (Li et al. 2001). Most of rotational/torsional studies of ground motion in earthquake engineering are so far still carried out by indirect measurements.

Indirect measurements of rotational motions using a seismo- (accelero-) meter array have been studied by several investigators (e.g., Niazi 1986; Oliveira and Bolt 1989; Spudich et al. 1995; Bodin et al. 1997; Singh et al. 1997; Huang 2003; Li et al. 2001). However, to the best of our knowledge, there is no com-

parison of array-derived rotation rate and direct measurement from rotational sensors described in the literature to date.

Here we present for the first time a comparison of rotational ground motions derived from seismic array data with those observed directly with a ring laser system. The goal of this study is to discuss the effects of noise and uncertainties in the array observations and their relevance to the derivation of rotation. In an era with more and more array type experiments and processing, the question of direct vs. array-type measurements becomes of interest in seismology, earthquake physics and geodesy. We will first present a synthetic study, in which we investigate the influence of various effects on array derived rotation rate. These effects are (1) unwanted signals (i.e., noise) in the horizontal components of translation, (2) uncertainty in seismometer calibration, and (3) uncertainty in station coordinates. Finally, we show the direct comparison of the vertical component of array-derived rotation rate with the ring laser gyroscope record for the M6.3 Al Hoceima, Morocco, earthquake of February 24, 2004. We conclude that the fit between these entirely independent measurements of the same wavefield property is surprisingly good.

2   The experiment

Following the successful observation of fully consistent rotational motions (Igel et al. 2005), a mobile seismic array experiment with eight stations (S1-8) was installed around the geodetic station Wettzell, Southeast Germany, the location of the ring laser. A ninth station was located in the geodetic station itself (12°52'44"E, 49°08'39"N), where a broadband seismometer (station WET, part of the German Regional Seismic Network, GRSN) is situated. The ring laser is located at a distance of approximately 250 m from the broadband seismometer. The radius of the seismic array is about 1.5 km, centered at station WET. The shallow subsurface structure consists of metamorphic rock basement covered by glacial till. The location of the array is shown in Figure 1.

Each seismic station consists of a three-component velocity sensor (Le3D-5s) having a flat response in ground velocity between 0.2 and 40 Hz, and a 400V/m/s generator constant. A 24-bit three-channel digital recorder was used to record the data. The sampling rate was 62.5 Hz and GPS time synchronization was achieved every 15 minutes. The experiment was running from December 2003 until early March 2004. The seismometers were buried in soft forest ground or they were deployed on outcropping large igneous rock boulders. The GRSN (WET) station is equipped with a STS-2 broadband instrument with a flat

response of to ground velocity from 8.33 mHz (120 s) to 50 Hz. The data are recorded with a sampling rate of 80 Hz.

The ring laser instrument, called 'G', consists of a He-Ne gas laser with a ultrahigh vacuum quality cavity enclosing an area of 16 m^2. The vertical component of rotation rate is recorded by this instrument with a sampling rate of 4 Hz. The G ring laser has a resolution of 9×10^{-11} rad/s/Hz (Schreiber et al. 2003). Further information on the ring laser instrument is given in Schreiber et al. (to appear). Several teleseismic earthquake events were observed during this experiment. However, very few of these events were recorded with high signal-to-noise ratio by both the ring laser system and the seismic array. We focus here on the event with the highest signal-to-noise ratio.

3 Observations and processing

The earthquake that will be investigated occurred on February, 24, 2004 at 02:27:46.2 (GMT). The epicenter was near the Mediterranean city of Al Hoceima (35.235° N, 3.963° W) about 295 km North-East from Rabat, Morocco. This earthquake occurred near the eastern end of the Rift mountain belt, which is part of the boundary between the African and Eurasian plates. The distance between the epicenter and the seismic network was about 2055 km (18.5∘). This M6.3 earthquake was recorded simultaneously by the array stations S1-S8, the broadband station (WET) and the ring laser. The array and broadband data are restituted by applying their seismometer response function. Figure 2 shows the restituted horizontal components of velocity seismograms, including broadband (WET) data. These components are needed to calculate the horizontal space derivatives necessary for the estimation of the vertical component of rotation rate. All the seismograms, including the broadband data are bandpass filtered from 0.03 to 0.5 Hz. As expected – after correction of the instrument response – for an earthquake at such an epicentral distance, considering the frequency band and the size of the array, there is almost perfect match in amplitude and waveform between the array seismograms and the broadband sensor despite their very different instrument characteristics. The maximum amplitude of the velocity was about 0.8×10^{-4} and 1.2×10^{-4} m/s for East-West and North-South components, respectively. However, a certain level of noise is visible for some of the stations (e.g., S4+5). One of the key questions to be addressed here is how such noise affects the array-derived rotational motions. In the following, we briefly describe how rotation rate can be derived from the horizontal components of array seismograms, and then apply the method to synthetic and observed

seismograms.

4   Deriving rotation from seismic array data

The relation between rotational and translational motions is obtained trough the application of the curl operator $\nabla \times$ to the seismic wave field $\vec{v}(x, y, z)$ by:

$$\begin{pmatrix} \omega_x \\ \omega_y \\ \omega_z \end{pmatrix} = \frac{1}{2} \nabla \times \vec{v} = \frac{1}{2} \begin{pmatrix} \partial_y v_z - \partial_z v_y \\ \partial_z v_x - \partial_x v_z \\ \partial_x v_y - \partial_y v_x \end{pmatrix}. \tag{1}$$

This implies that – in principle – the rotational components can be estimated if we are able to calculate the spatial derivatives of ground velocity. As is well known from numerical mathematics, partial derivatives (in one dimension) can be approximated introducing information from two or more points sampling the vector field and solving an approximate system of linear equations. In what follows, we will restrict ourselves to the vertical component of rotation, as it is the component the ring laser is measuring. The simplest method to approximate the derivatives of the horizontal components of motion is to subtract two recordings of ground displacement (velocities, acceleration) and divide by their distance (finite-difference approximation). This can be done especially when the points are distributed regularly in an ideal cross shaped array (e.g., Huang 2003). In this paper we apply a standard geodetic method to estimate the static displacement for calculating the space derivatives. This has been previously used by Spudich et al. (1995) to study the dynamic deformation induced by the $M7.4$ Landers earthquake of June 28, 1992, derived from the UPSAR array in Parkfield, California. This method was also used by Bodin et al. (1997) to study dynamic deformations of shallow sediments in the Mexico basin.

We briefly describe this method in the following. At the free surface boundary, it can be shown that the time-dependent displacement gradient matrix G can be estimated from ground displacement components u_i $(i = 1..N)$ recorded at N stations by solving the set of equations:

$$d_i = GR_i$$

$$= \begin{pmatrix} \partial_x u_x & \partial_y u_x & \partial_z u_x \\ \partial_x u_y & \partial_y u_y & \partial_z u_y \\ \partial_z u_x & -\partial_z u_y & -\eta(\partial_x u_x + \partial_y u_y) \end{pmatrix} R_i, \tag{2}$$

where, $\eta = \lambda(\lambda + 2\mu)$, λ and μ are the Lamé parameters, $d_i = u_i - u_0$, $R_i = r_i - r_0$, u_i, r_i, and u_0, r_0, are the displacements at the coordinates of the

i^{th} station and the reference station (subscript 0), respectively. At least three stations have to be used to determine the horizontal displacement gradient using this method. Assuming the array stations were located at the same elevation, the vertical component of rotation rate ω_z can be obtained by solving equation (2) using three stations (S_i, S_j, S_k):

$$\omega_z = \frac{1}{2A} \left(\left[b_i u_{i_y} + b_j u_{j_y} + b_k u_{k_y} \right] - \left[c_i u_{i_x} + c_j u_{j_x} + c_k u_{k_x} \right] \right), \qquad (3)$$

where A is the area bounded by the station S_i, S_j and S_k, $b_i = (y_k - y_j)/2$, $c_i = (x_k - x_j)/2$, and b_j and c_j obtained by index circular permutation. Here $(x_i, y_i),(x_j, y_j)$ and (x_k, y_k) are coordinates of stations S_i, S_j and S_k, respectively. When more than three stations are used, equation (2) can be solved using a least-squares procedure. More details can be found in Spudich et al. (1995).

5 Spatial characteristics of the seismic array wavefield: observations vs. simulation

One of the key questions in this study is to understand the effects of various sources of uncertainties in the array observations on the array-derived rotational ground motions. The method described above is therefore first tested against a synthetic array data set. Complete theoretical seismograms for translations and rotations were calculated using a recent 3-D global tomography model (Ritsema and Van Heijst 2000), and a point-source approximation of the Al Hoceima event. Seismograms were calculated using the spectral-element method (Komatitsch and Tromp 2002a,b) that was extended to allow outputting the curl of the velocity-wave field (i.e., rotation rate). The numerical simulation for this short epicentral distance was carried out with a spatial and temporal resolution allowing an accurate wavefield down to periods of 5 seconds (Schuberth et al. 2003). The receivers were located at the same positions as our array seismometers. Figure 3 shows the time histories of the horizontal components of the synthetic ground velocity and superposition of all traces in a short time window. Due to the epicentral distance ($\sim$ 2000 km) and the considered spatial and temporal wavelengths, the waveforms are almost identical across the array.

In the following we aim at investigating the effects of noise at some of the seismic stations. As the minimum number of stations to determine the spatial gradient is three, we choose to estimate rotations from (sub-) triangular array sections to investigate (1) the uniformity of the derived rotation across the ar-

ray and (2) to identify observed array sections with high noise level, coupling differences, or instrumental problems. Because of the spatial wavelengths considered in the synthetic wavefield, we expect the rotational motions to be close to uniform across the array. Figure 4 shows four pairs of the vertical component of array-derived rotation rate calculated using combinations of three stations of the outermost array stations (S5, S6, S7 and S8) with WET as the reference station (gray line) superimposed with synthetic rotation rate (black line) at the center of the array (WET). The normalized correlation coefficients (maxima) are given above the trace pairs. The stations used to derive the vertical component of the array-derived rotation rate are given in the bottom of each trace pair. As expected with noise-free synthetics, the array-derived rotation rate matches almost exactly the rotation rate calculated at the central station WET (corr. coeff. > 0.99).

We now perform the same exercise with the observations of the Al Hoceima event. In Figure 5, the direct observations of rotation rate with the ring laser (black line) at the center of the array is compared with the array-derived rotation rate (gray line) using four different sub-triangles. First, we observe that the array-derived rotation rate (using three stations only) varies substantially for the different triangles suggesting considerable amount of noise across the array. Second, while in one sub-triangle (S6-WET-S7) the phase match is quite good in the most part of the time series, the amplitudes not matching so well, in another one (S5-WET-S8) the amplitudes are closer to the direct measurements, while this time the phases poorly match in general. These observations suggest that different sources of noise (amplitude, phase, etc.) seem to affect the various array stations.

Note that here we have deliberately taken the decision to use only three (of nine possible) stations to determine rotations in order to highlight noise in the data. In the final comparison all stations are used. Before investigating specific noise effects more systematically, we demonstrate that – assuming random noise added to the synthetic array seismograms – we reproduce a behavior similar to what is seen in the observations. We add 3% Gaussian white noise to all seismograms. Station 8, however, is additionally perturbed by 10% phase uncertainty in the x-component. The sub-triangle determination of rotation rate shown in Figure 6a now exhibits misfits similar to those of the observations in Figure 5. The sub-triangles containing the phase-perturbed seismometer (S8) compares poorly with the (noise-free) rotational signal at the center of the array. However, if we use all nine stations to determine the rotational signal, most of the random noise cancels out and the final array-derived rotation rate compares

8

well with the (noise-free) rotational signal at the center of the array (Figure 6b). This indicates that (random) errors in parts of the array data may cancel out when a sufficiently large number of stations is used. On the other hand, using only three stations for array-derived rotations may considerably increase the uncertainties with respect to final rotation estimates.

6 Effects of noise on array-derived rotations and comparison with directly measured rotation

In this section we will examine the effects of various levels of synthetic uncorrelated random noise, real background noise (extracted from observations), uncertainties in the position determinations and uncertainties in the seismometer gain on the array-derived rotation rate. The vertical component of rotation rate is calculated using all the data from the nine stations, as will be done when finally comparing with direct observations.

To study the effects of uncorrelated random noise in the array seismograms, we generate a Gaussian random signal with maximum amplitudes of 1%, 5%, and 10%, of the maximum amplitude of the horizontal component of the synthetic velocity seismograms. This random signal is added to the synthetic array data. The array-derived rotation rate from 25 random signal realizations is depicted in Figure 7 (gray) and compared with the noise-free exact rotation rate at the center of the array. The average root-mean-square (rms) difference of the array-derived rotation rate was 1.33%, 6.43%, and 12.87% for 1%, 5%, and 10% noise, respectively. With 10% noise the waveforms are severely distorted but the dominant phases are still well matched with peak amplitude errors similar to the noise percentage. With 5% noise the waveforms are affected by the low-frequency part of the random noise, while, with 1%, the differences between the curves is barely more than the thickness of the line.

The actual noise level in the observations can be estimated by taking signals prior to the first arriving energy of the event under investigation. In the following, noise signals are extracted from the observations some minutes before the first arriving energy for each of the nine stations. These signals are added to the synthetic array seismograms and the rotational signal is estimated and compared to the noise-free rotational signal at the center of the array. The background noise is on average about 3% of the peak amplitude of the velocity seismograms. The results are shown in Figure 8 (top). The rms-difference of the array-derived rotation rate with respect to the true signal is 3.58%. These

results suggest that with the observed noise level – in the absence of other errors (e.g., systematic errors such as timing, filter problems, etc.) – it should be possible to derive the rotational signal from the array observations with similar certainty (within a few percent).

Array station coordinates are essential for the calculation of the array-derived rotational signal. In our experiment we use a portable GPS receiver for synchronizing the time and for the determination of the stations' coordinates. The problem with this kind of GPS is their low accuracy in position determination. In our experiment, the coordinate precision was affected by the nearby presence of buildings or trees. As a consequence, the uncertainty in seismometer's position in our experiment is several meters.

To estimate the effect of position uncertainties, we introduce random position errors from -30 to +30 meters in the x and y coordinates and calculate the rotation rate for 25 such realizations. The results are shown in Figure 8 (bottom). The average rms-difference of the array-derived rotation rate is 0.38%. From this we conclude that the uncertainties introduced through the GPS measurements are unlikely to deteriorate the final array-derived estimates of the rotational signal.

Amplitude errors may be introduced through local site effects at the stations and/or instrumental problems. To investigate the effects we randomly modify the overall amplitude of the synthetic data by a factor of 1%, 5%, and 10%. The calculated rotation rate from 25 realizations in each case is depicted in Figure 9. The rms-difference of the array-derived rotation rate is 0.34%, 0.51%, and 1.70%, for 1%, 5%, and 10% amplitude uncertainty in each of the array components, respectively. Even though this test is somewhat simplified, the results suggest that random (constant/static) amplitude errors are unlikely to alter the final results – given our array configuration – significantly.

Finally, we derive the array-derived rotation rate for the Al Hoceima event from the horizontal seismograms of all nine array stations (Figure 2). In Figure 10 we show the comparison between the array-derived rotation rate with ring-laser based direct measurements of the same wave field quantity. We stress here that the traces are compared with absolute amplitudes. The overall rms-difference is 3.72%. The maximum normalized correlation coefficients are given below each seismogram. The best correlation coefficient is 0.97 in the Love wave time window. In the early part of the seismogram, the fit is worse. This is probably due to the low amplitudes compared to the peak amplitudes of the Love wave train. In addition, this time window contains the highest frequencies and we expect the uncertainties to increase with frequency. The match between

the direct and array-derived rotation rate is almost perfect in the three-minute time window containing the fundamental and higher mode Love waves with correlation coefficients above 0.95. The overall fit is worsening towards the end of the signal due to decreasing signal-to-noise ratio. The surprisingly good fit of those entirely different approaches to measuring the rotational part of the wave field confirms the quantitative results of the synthetic study, particularly the fact that the final similarity is obtained thanks to the relatively large number of seismic array stations given the observed noise levels.

7 Discussion and Conclusions

Recently, the interest in the observation of rotational ground motions has increased after this type of motion has been neglected for decades despite the fact that theoreticians suggest it should be observed (e.g., Aki and Richards 2002). While instruments that directly measure ground rotations are still being developed (e.g., Schreiber et al. to appear), there is more and more evidence that rotational motions my indeed be useful for the understanding of earthquake source processes (Takeo and Ito 1997), deriving the complete ground motion from rotations and translations (Trifunac and Todorovska 2001), or in understanding local strong-motion effects due to rotations (Castellani and Zembaty 1996). Rotational motions can be derived from surface measurements of the horizontal components of at least three stations. This was investigated in several studies (e.g., Bodin et al. 1997; Huang 2003). However, because at that time appropriate instruments for the direct measurement of rotations were not available, it was impossible to assess the accuracy of these measurements. In the past years, ring laser technology provided the technical means to observe rotational motions around the vertical axis with the required precision in broadband seismology. The full consistency of the ring laser observations with broadband translational motions was shown by Igel et al. (2005) and further studies by Cochard et al. (to appear) and Schreiber et al. (2003).

Using ring-laser technology we present here the first comparison of seismic array-derived rotations with direct measurements. The goal of this study was (1) to quantify the accuracy with which rotations can be derived from seismic array data; (2) to investigate the effects of noise; and (3) to discuss issues concerning array versus direct measurements of rotations. The seismic array experiment that was carried out between December 2003 and March 2004 with a radius of $\approx$ 1.5 km around the ring laser instrument was to some extent sub-optimal because (1) the seismic equipment we used (LE3D-5s) is not designed for teleseismic

studies and long-period signals, and (2) as far as the array geometry goes, the emphasis was on having a shape as close to a regular "finite-difference stencil" as possible resulting in heterogeneous site conditions (from muddy forest ground to outcropping granite boulders). These conditions and the high noise levels on the horizontal components resulted in a data set in which only very few large teleseismic events were usable for the rotation estimates.

Nevertheless, in the light of the experimental circumstances the fit between array-derived rotations and direct ring laser measurements (Figure 10) is stunning, given the observation of a wave field property (rotation around a vertical axis) with entirely different physical methodologies. We expected that errors in individual station observations play a stronger role particular when calculating spatial derivatives. The estimated noise level in the array seismograms was around 3% and it is interesting to note that a quantitatively similar misfit between array-derived rotation and direct measurements is observed for the most dominant signals (Love waves). These results indicate that – given accurate measurements of translational motions in an array of appropriate size and number of stations – the array-derived rotation rate may be very close to the "true" rotational signal that would be measured at the center of the array (or the specific reference station). However, it is important to note that – given the observations described in Figure 5 – it may be dangerous to use only the minimally required three stations as even relatively small noise levels may deteriorate the rotation estimates.

While the results suggest that the observation of array-derived rotations is feasible, it is important to note that we considered a fairly long-period signal in this study. Errors will certainly be more pronounced for earthquakes with shorter epicentral distances and higher-frequency wave fields. In the light of this, the necessity to develop field-deployable rotational sensors with the appropriate resolution for use in local and regional seismology remains an outstanding issue.

8   ACKNOWLEDGMENTS

References

K. Aki and P. G. Richards. *Quantitative Seismology.* University Science Books, 2nd edition, 2002.

C. Bassin, G. Laske, and G. Masters. The current limits of resolution for surface wave tomography in north america. *EOS Trans. Amer. Geophys. Union*, 81: F987, 2000.

P. Bodin, J. Gomberg, S. K. Sing, and M. Santoyo. Dynamic deformations of shallow sediments in the valley of Mexico, part I: Three-dimensional strains and rotations recorded on a seismic array. *Bull. Seismol. Soc. Am.*, 87:528–539, 1997.

A. Castellani and Z. Zembaty. Comparison between earthquake spectra obtained by different experimental sources. *Engng Struct.*, 18:597–603, 1996.

A. Cochard, H. Igel, A. Flaws, B. Schuberth, J. Wassermann, and W. Suryanto. Rotational motions in seismology: theory, observation, simulation. In Teisseyre et al., editor, *Earthquake source asymmetry, structural media and rotation effects.* Springer Verlag, to appear.

B.-S. Huang. Ground rotational motions of the 1999 Chi-Chi, Taiwan earthquake as inferred from dense array observations. *Geophys. Res. Lett.*, 30: 1307–1310, 2003.

H. Igel, U. Schreiber, A. Flaws, B. Schuberth, A. Velikoseltsev, and A. Cochard. Rotational motions induced by the M 8.1 Tokachi-oki earthquake, September 25, 2003. *Geophys. Res. Lett.*, 32:L08309, 2005.

D. Komatitsch and J. Tromp. Spectral-element simulations of global seismic wave propagation, Part I: Validation. *Geophys. J. Int.*, 149:390–412, 2002a.

D. Komatitsch and J. Tromp. Spectral-element simulations of global seismic wave propagation, Part II: 3-D models, oceans, rotation, and gravity. *Geophys. J. Int.*, 150:303–318, 2002b.

H. Li, L. Sun, and S. Wang. Improved approach for obtaining rotational components of seismic motion. In *Transactions, SMiRT 16*, Washington DC, 2001.

D. P. McLeod, G. E. Stedman, T. H. Webb, and U. Schreiber. Comparison of standard and ring laser rotational seismograms. *Bull. Seismol. Soc. Am.*, 88: 1495–1503, 1998.

T. Moriya and R. Marumo. Design for rotation seismometers and their calibration. *Geophys. Bull. Hokkaido Univ.*, 61:99–106, 1998.

M. Niazi. Inferred displacements, velocities and rotations of a long rigid foundation located at El centro differential array site during the 1979 Imperial Valley, California earthquake. *Earthquake Eng. Struct. Dyn.*, 14:531–542, 1986.

R. L. Nigbor. Six-degree-of-freedom ground-motion measurement. *Bull. Seismol. Soc. Am.*, 84:1665–1669, 1994.

C. S. Oliveira and B. A. Bolt. Rotational components of surface strong ground motion. *Earthquake Eng. Struct. Dyn.*, 18:517–26, 1989.

A. Pancha, T. H. Webb, G. E. Stedman, D. P. McLeod, and K. U. Schreiber. Ring laser detection of rotations from teleseismic waves. *Geophys. Res. Lett.*, 27:3553–3556, 2000.

E. J. Post. Sagnac effect. *Rev. Mod. Phys.*, 39:475–493, 1967.

J. Ritsema and H. J. Van Heijst. Seismic imaging of structural heterogeneity in earth's mantle: Evidence for large-scale mantle flow. *Science Progress*, 83: 243–259, 2000.

G. A. Sanders, M. G. Prentiss, and S. Ezekiel. Passive ring resonator method for sensitive inertial rotation measurements in geophysical and relativity. *Opt. Lett.*, 6:569–571, 1981.

K. U. Schreiber, T. Klügel, and G. E. Stedman. Earth tide and tilt detection by a ring laser gyroscope. *J. Geophys. Res.*, 108:2132, 2003.

U. Schreiber, H. Igel, A. Cochard, A. Velikoseltsev, A. Flaws, B. Schuberth, W. Drewitz, and F. Müller. The GEOsensor project: rotations – a new observable for seismology. In Rummel et al., editor, *Geotechnologies-book*. Springer Verlag, to appear.

B. Schuberth, H. Igel, J. Wassermann, A. Cochard, and K. U. Schreiber. Rotational motion from teleseismic events – modelling and observations. *EOS Trans. Amer. Geophys. Union*, pages Fall Meet. Suppl. Abstract S42D–0200, 2003.

S. K. Singh, M. Santoyo, P. Bodin, and J. Gomberg. Dynamic deformations of shallow sediments in the valley of Mexico, part II: Single station estimates. *Bull. Seismol. Soc. Am.*, 87:540–550, 1997.

P. Spudich, L. K. Steck, M. Hellweg, J. B. Fletcher, and L. M. Baker. Transient stresses at Parkfield, California, produced by the M 7.4 Landers earthquake of June 28, 1992: Observations from the UPSAR dense seismograph array. *J. Geophys. Res.*, 100:675–690, 1995.

G. E. Stedman, Z. Li, and H. R. Bilger. Sideband analysis and seismic detection in a large ring laser. *Appl. Opt.*, 34:7390–7396, 1995.

M. Takeo. Ground rotational motions recorded in near-source region of earthquakes. *Geophys. Res. Lett.*, 25:789–792, 1998.

M. Takeo and H. M. Ito. What can be learned from rotational motions excited by earthquakes. *Geophys. J. Int.*, 129:319–329, 1997.

R. Teisseyre, J. Suchcicki, K. P. Teisseyre, J. Wiszniowski, and P. Palangio. Seismic rotation waves: basic elements of theory and recording. *Annali di Geofisica*, 46:671–685, 2003.

M. D. Trifunac and M. I. Todorovska. A note on the useable dynamic range of accelerographs recording translation. *Soil Dyn. and Earth. Eng.*, 21:275–286, 2001.
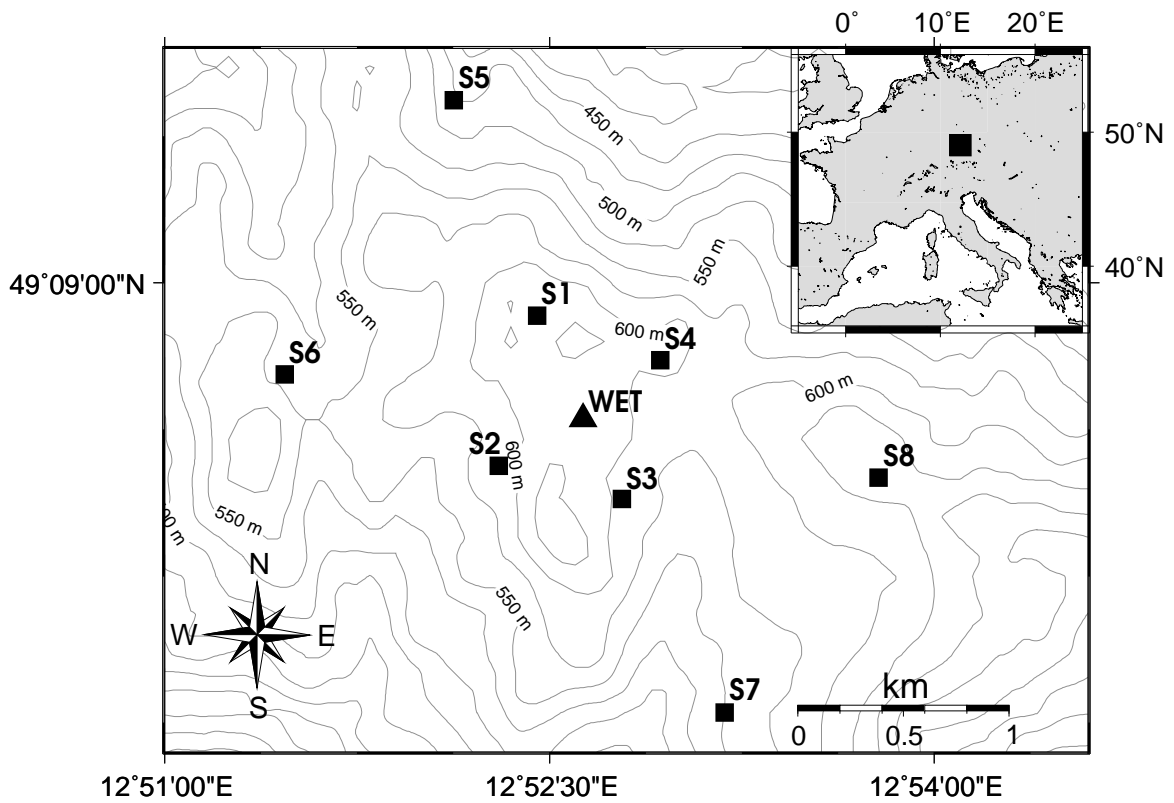
Figure 1: Location of the array experiment. The ring laser and GRSN (German Regional Seismic Network) broadband station (WET) are located at the center of the array marked by a triangle. The ring laser and the broadband seismometer are separated by approximately 250 m.
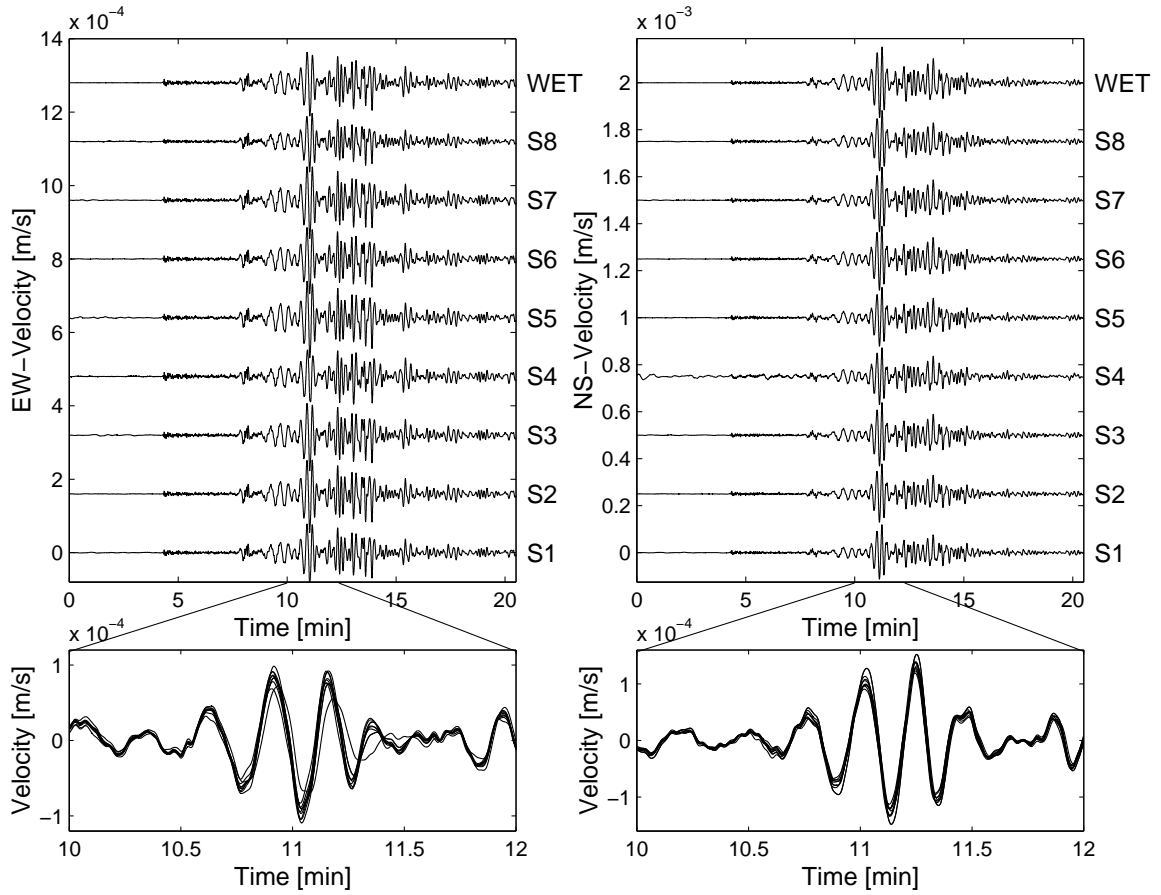
Figure 2: Velocity seismograms for the M6.4 Al Hoceima Morocco earthquake of February 24, 2004, recorded by the array. A superposition of all seismograms in a 2-minute time window is shown in the lower part. All seismograms, including the broadband seismogram (WET, top), are restituted and bandpass filtered from 0.03 Hz to 0.5 Hz.
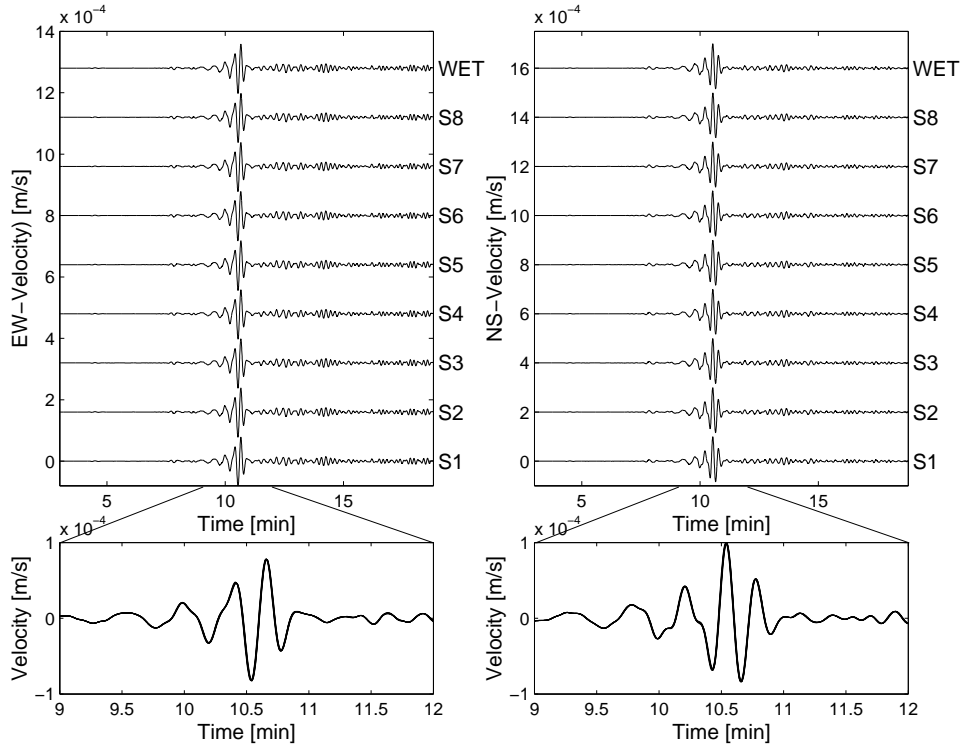
Figure 3: Synthetic velocity seismograms for the $M6.4$ Al Hoceima Morocco earthquake of February 24, 2004, for all the array's station as well as the central station (WET), calculated for a 3-D mantle model (Ritsema and Van Heijst 2000) and a recent crustal model (Bassin et al. 2000). The seismograms are calculated using the spectral element method (Komatitsch and Tromp 2002a,b) and bandpass filtered from 0.03 Hz to 0.5 Hz.
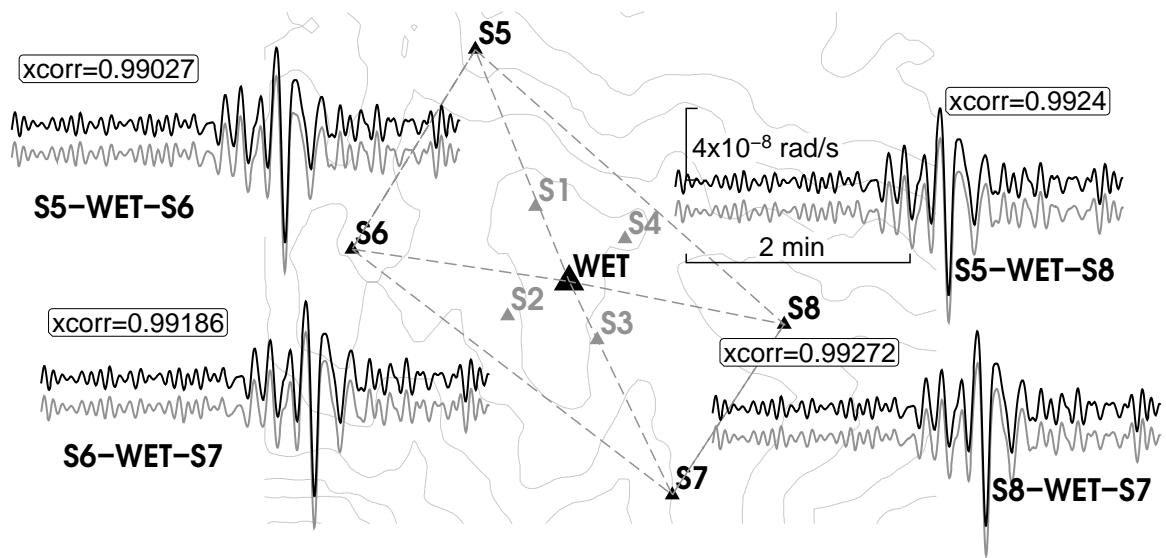
Figure 4: Synthetic test of uniformity of rotation rate across the array. Vertical component of rotation rate at the array center (black lines) and array-derived rotation rate (gray lines) calculated using three stations for four different sub-triangles (indicated in each panel). The normalized correlation coefficients are given for each trace pair.
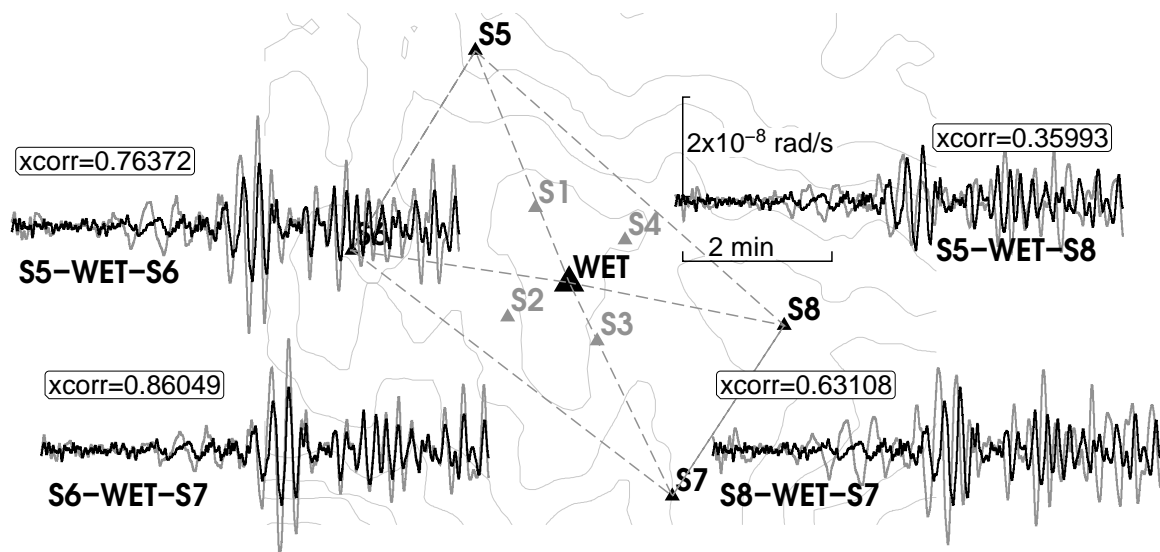
Figure 5: Non-uniformity of array-derived rotation rate (gray lines) across the array in different sub-triangles, as noted in each panel, for real data compared with the direct rotational measurements at the center of the array by a ring laser (black lines). The normalized correlation coefficients are given for each trace pair.
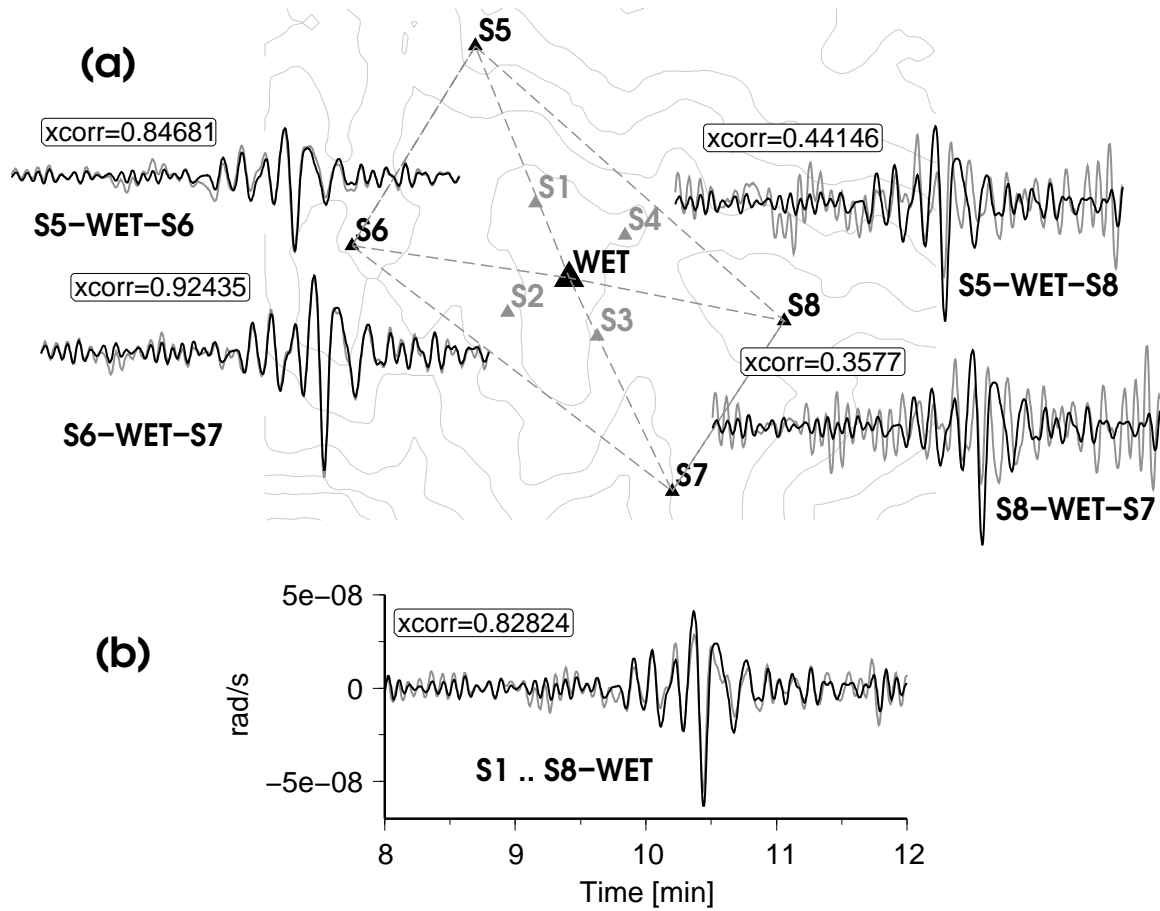
Figure 6: Non uniformity of array-derived rotation rate across the array for different sub-triangles for synthetic data with a single phase-disturbed station (S8 – by 10%) and 3% of random noise added for all stations. (a) Vertical component of rotational motions at the center of the array (black lines) superimposed with array-derived rotation rate (gray lines) calculated using three stations, as indicated. (b) Vertical component of array-derived rotation rate (gray) is calculated from all nine stations and compared with the true rotation (black line). The normalized correlation coefficients are given for each trace pair.
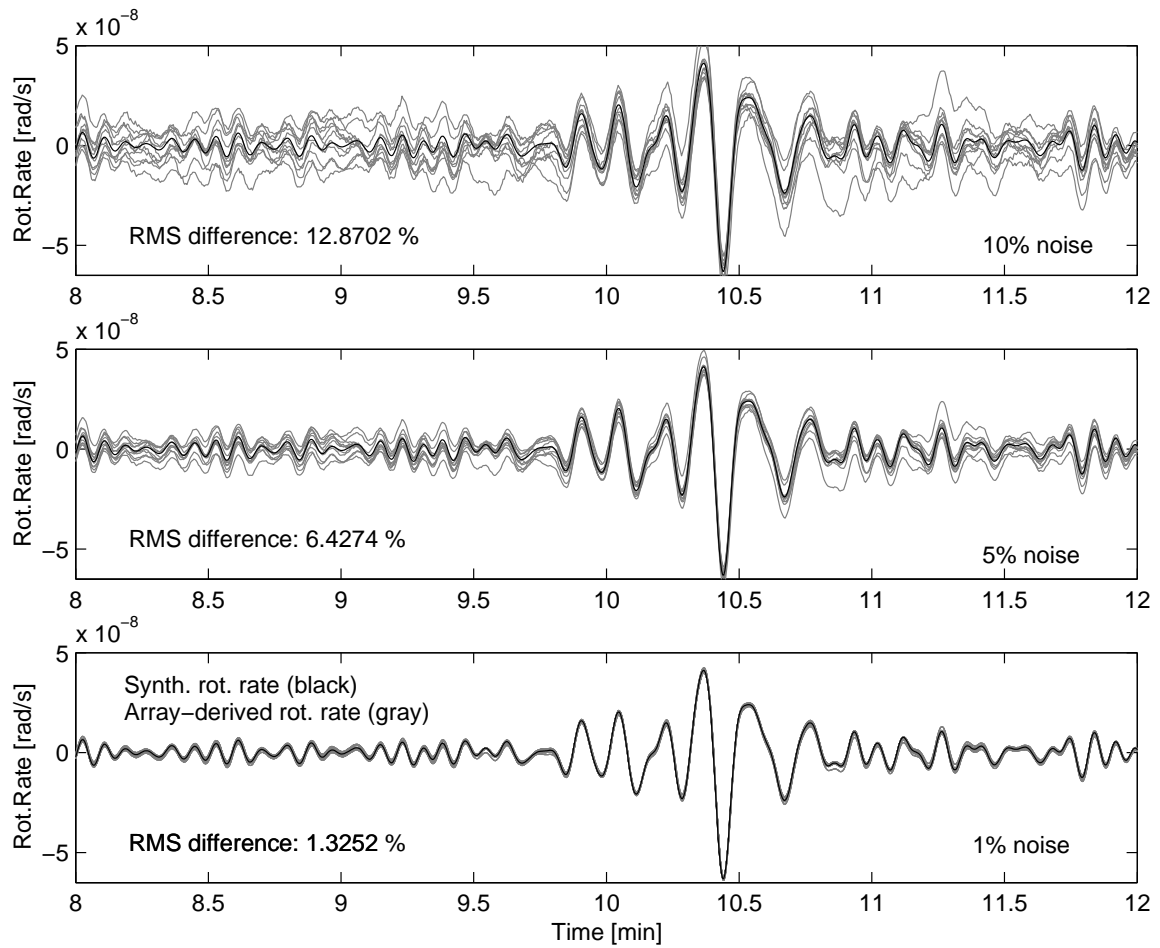
Figure 7: Vertical component of array-derived rotation rate from synthetic data with Gaussian random noise (with 25 noise realizations) (gray line), superimposed with the noise-free synthetic rotation rate (black line). The amount of noise is 10%, 5% and 1%, from top to bottom. Only for 1% noise is the rotation rate reasonably well retrieved.
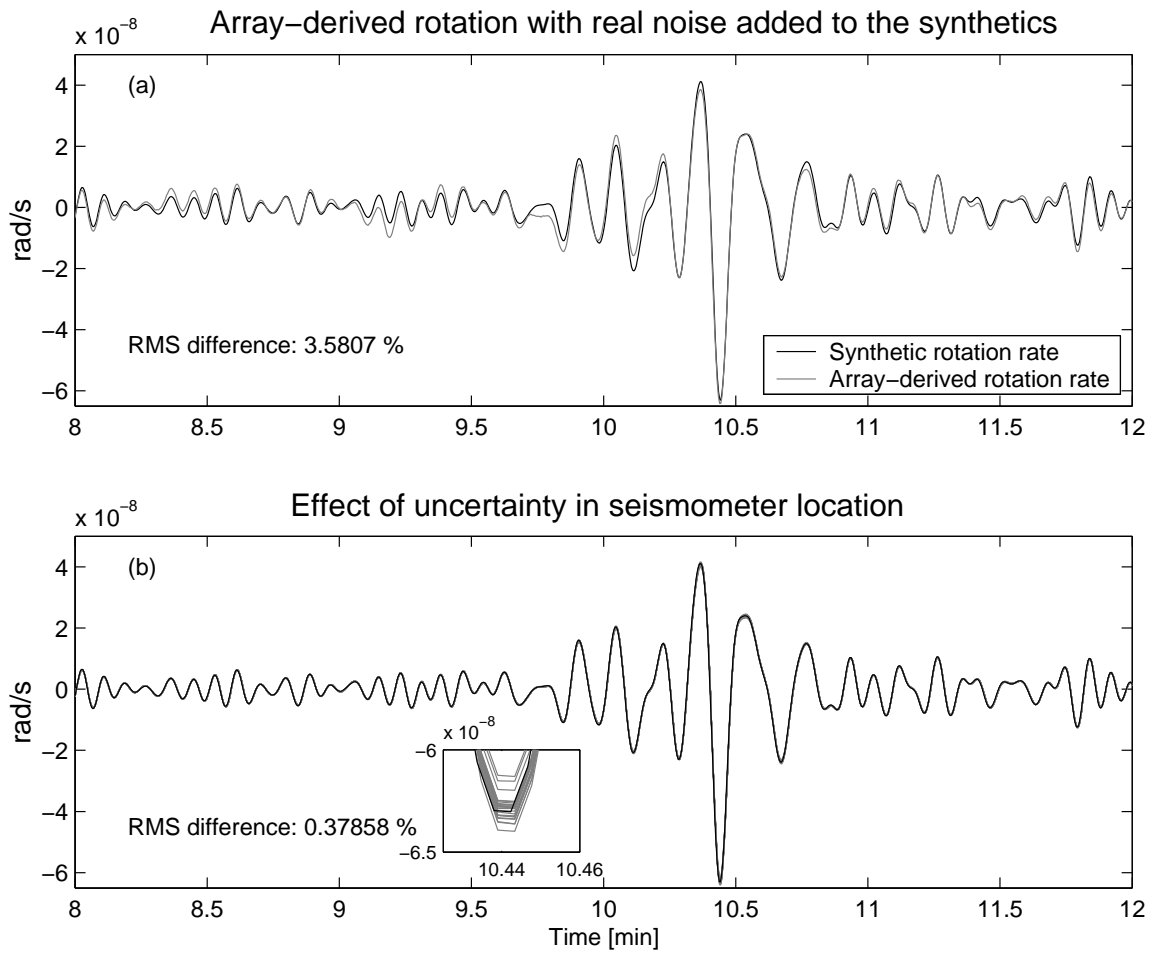
Figure 8: Top: Vertical component of array-derived rotation rate from synthetic data with real noise taken from the observed seismograms several minutes before the event started. This shows that noise level is not the only cause of the poor results seen in Figure 4. Bottom: Effects of a ±30 m maximum error in seismometer position on the derivation of rotation rate for 25 realizations; this shows that inaccuracies in GPS location in unlikely to affect our results.
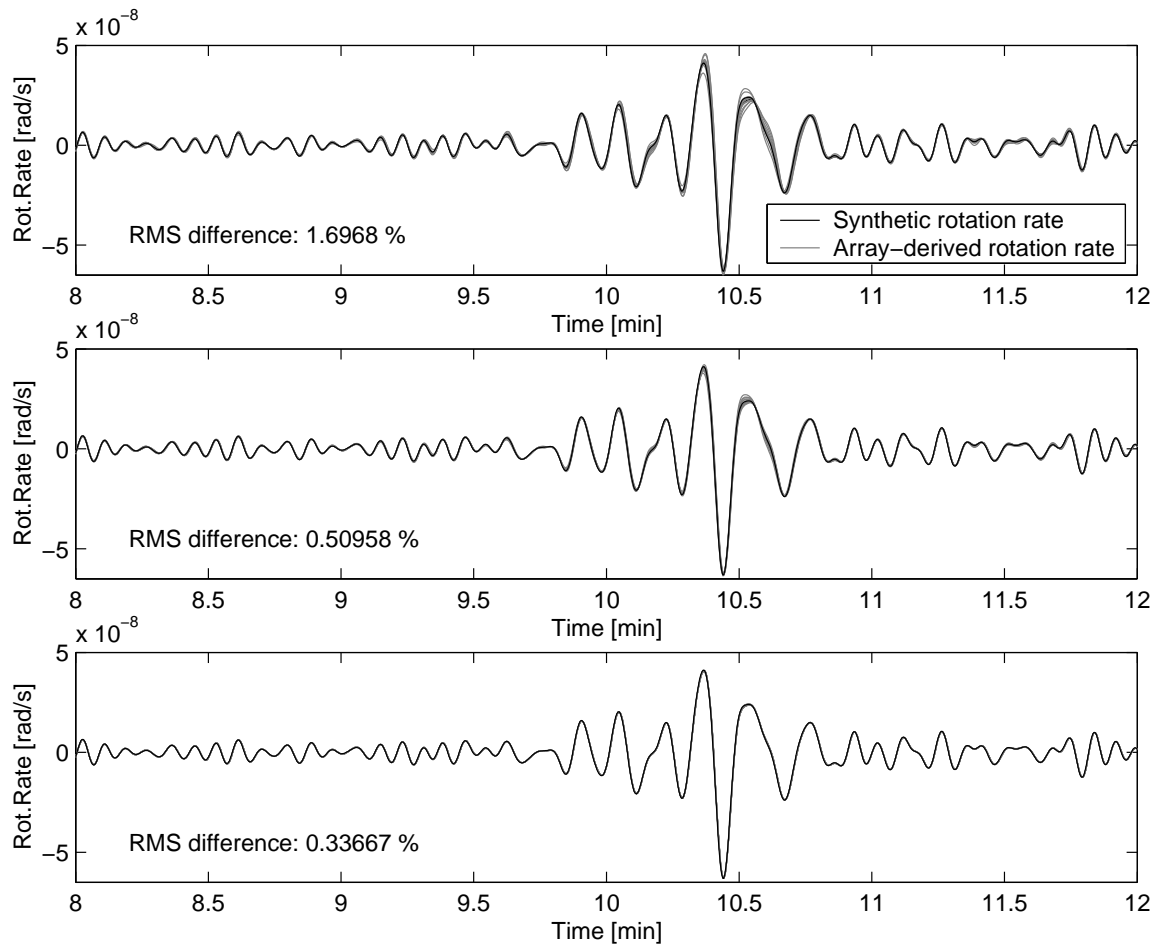
Figure 9: Vertical component of array-derived rotation rate for synthetic data with amplitude uncertainty of 10%, 5%, and 1% (top to bottom), from 25 realizations (gray lines) superimposed with synthetic rotation rate (black line).
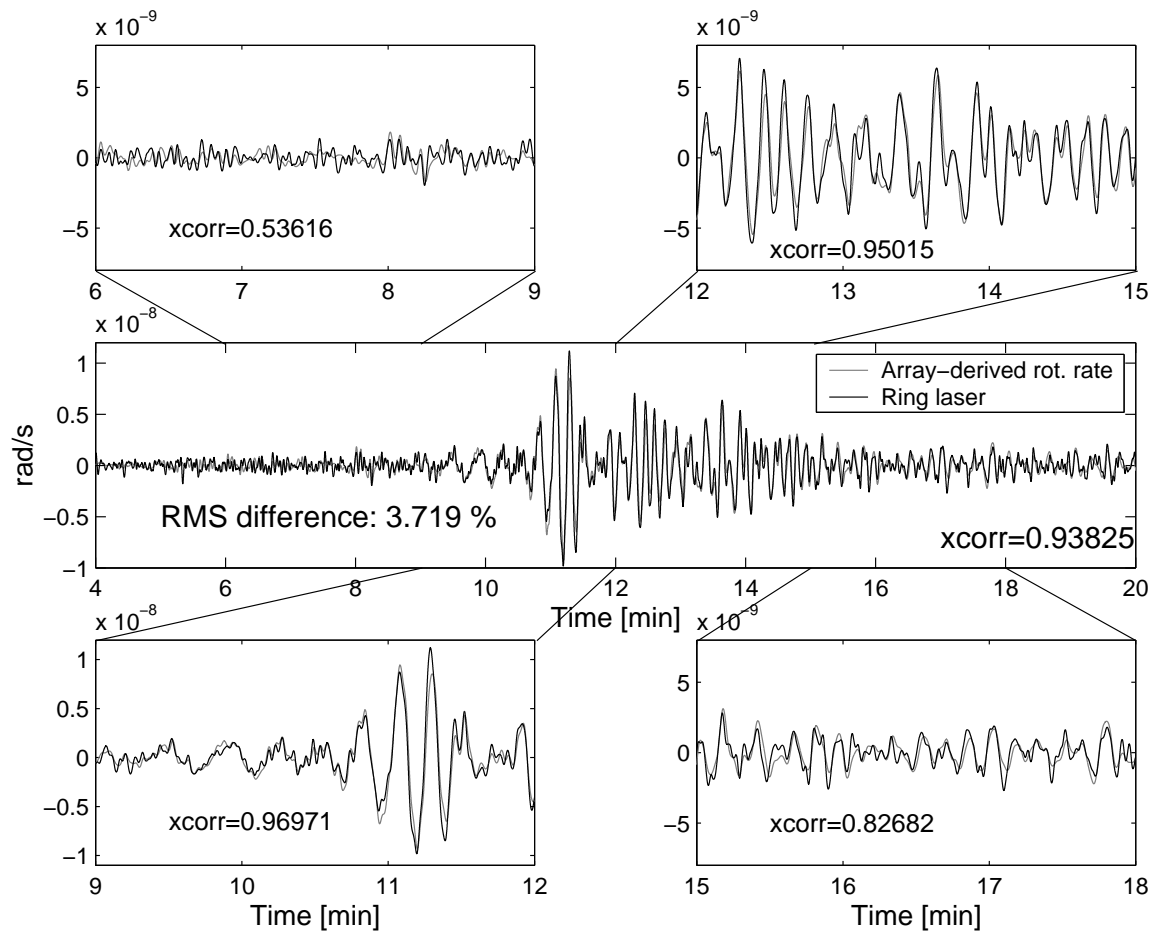
Figure 10: Vertical component of array-derived rotation rate from real array data set (gray line) superimposed with ring laser data (black line). Nine stations including the broadband data are used to calculate the array-derived rotational signal. Both traces are bandpass filtered from 0.03 Hz to 0.3 Hz.